# ADDRESSING SYSTEM INTEGRTAION ISSUES REQUIRED FOR THE DEVELOPMENT OF DISRIUBTED WIND-HYDROGEN ENERGY SYSTEMS

**Department of Energy Experimental Program to Stimulate Competitive Research (DOE/EPSCoR)**
**EPSCoR State – DOE National Laboratory Partnership Awards**

**DOE Grant No. DE-FG02-04ER46115**

**Final Technical Report**

**Submitted by**
**Dr. Michael D. Mann**
**University of North Dakota**
**Grand Forks, ND**

**April 1, 2008**

**ADDRESSING SYSTEM INTEGRTAION ISSUES REQUIRED FOR THE DEVELOPMENT OF DISRIUBTED WIND-HYDROGEN ENERGY SYSTEMS**
**EPSCoR State – DOE National Laboratory Partnership Award**
**Final Technical Report**

Wind generated electricity is a variable resource. Hydrogen can be generated via electrolysis as an energy storage media and fuel, but is costly. Advancements in power electronics and system integration are needed to make electrolysis a more viable system. Therefore, the long-term goal of the efforts at the University of North Dakota is to merge wind energy, hydrogen production, and fuel cells to bring emission-free and reliable power to commercial viability. The primary goals of this research include:

1. Expand system models as a tool to investigate integration and control issues.
2. Examine long-term effects of wind-electrolysis performance from a systematic perspective.
3. Collaborate with NREL to design, integrate, and quantify system improvements by implementing a single power electronics package to interface "wild" AC to PEM stack DC requirements.

**PROJECT TEAM:**

Dr. Michael D. Mann, Professor, Chemical Engineering
Dr. Hossein Salehfar, Professor, Electrical Engineering
Dr. Eduardo Hernandez Pacheco, Postdoctoral Fellow, Chemical Engineering, currently with Intel
Dr. Kevin Harrison, Doctoral Student, Engineering – currently with NREL
Andrew Peters, Doctoral Student, Engineering – currently with Clipper Windpower Development Co.
Christian Biaku, Doctoral Student, Engineering
Nilesh Dale, Doctoral Student, Engineering, expected graduation December 2008
Taehee Han, Doctoral Student, Engineering, expected graduation August 2009
Clay Anderson, Undergraduate Student, Electrical Engineering
Charles Nyberg, Undergraduate Student, Chemical Engineering
William Lovelace, Undergraduate Student, Electrical Engineering
Christopher Dewall, Undergraduate Student, Electrical Engineering

**STATUS:**

The funding provided through this grant has allowed the University of North Dakota (UND) to answer several important questions with regard to the development of distributed wind-hydrogen systems. These findings are summarized in this report and presented in more detailed in the papers developed during the project and referenced at the end of this report. More important than these findings has been the development of an experimental system at UND that can be used to continue to train students at all levels in the area of PEM fuel cells, electrolysis, and electrochemical compression. Equally important is the training already provided to six students as a part of their doctoral program and four undergraduate students as a part of their senior design projects. The training provided to these students will allow them successfully advance the implementation hydrogen as a viable energy source.

**PROGRESS AGAINST SCHEDULE/MILESTONES STATED IN DOE/EPSCOR PROPOSAL**

In this section, the deliverables that were stated in our original proposal are presented in italics followed by a detailed discussion of the progress toward meeting each deliverable.

1. *Detailed and empirically verified models of the following subcomponents and integrated systems examining wind power profiles, system sizing, operating conditions, hydrogen storage, dispatchable load scenarios, and economics.*

- *electrolyzer*
- *fuel cell*
- *hydrogen storage*

The task of the PEM fuel cell/electrolysis team is to develop improved models for performance studies of PEM fuel cells and electrolysis units in hybrid networks. A part of this goal involved developing models compatible with NREL's RPM-SIM software. Apart from working with RPM-SIM, these models have the capability to run independently for PEM fuel cell and electrolysis studies under different operating conditions of temperature, pressure and humidity. Modeling results for the fuel cell and electrolysis modules are summarized here. Details will be presented in the open literature (see listing at the end of this report)

**Fuel Cell Model (Proton Exchange Membrane Fuel Cell)**

The ionic conductivity of a proton exchange membrane fuel cell (PEMFC) is directly related to the water content in the fuel cell membrane. In other words, the membrane used needs to be hydrated at all times in order to reduce ohmic losses and increase the performance of the cell. We have developed an along-the-channel model that determines the amount of water inside the gas channels of a conventional PEMFC, and temperature distributions for both electrodes. The accurate prediction of the water content in the system is important for maintaining 1) a high protonic conductivity in the membrane, 2) a hydrated anode, and 3) a non-flooded cathode. These three effects involve an efficient water management in a PEMFC which leads to an optimal design. The model also calculates the current distribution at a specific voltage and ultimately, the power. The model will be used as a tool for optimization and design.

A co-flow array is used in the model. Fuel and oxidant enter the same side of the cell and move parallel to each other along the channel. Downstream, the fuel and oxidant are consumed due to the elctrochemical reactions. The model consists of eight differential equations and one algebraic equation to calculate the mass fluxes of $H_2$, $O_2$, and $H_2O_v$ at the anode and cathode and anode and cathode temperatures. Highlights of the modeling effort include:

- Along-the-channel-model,non-isothermal, single-phase model.
- In general the model developed allows the determination of the voltage-current characteristics of the fuel cell (Fig. 1).
- In particular the model is used to analyze the distribution of temperature, current and water content along the channels of a fuel cell stack (Fig. 2).
- The information provided by the model is used to effectively improve water management in the cell and therefore the overall performance of the system.

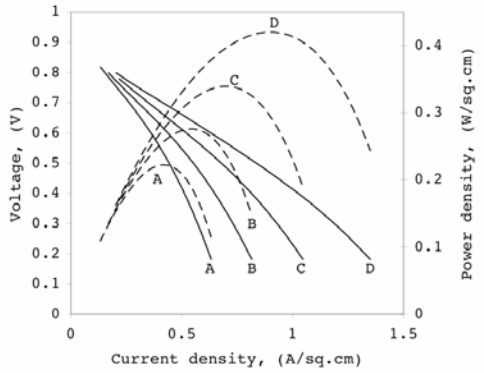


Fig.1 Shows the IV-characteristics of the fuel cell at different temperatures; (A) 60 C, (B) 70 C, (C) 80 C, (D) 90 C.

**Electrolyzer Model (Proton Exchange Membrane Electrolyzer)**

Critical proton exchange membrane (PEM) electrolyzer parameters like membrane conductivity, thickness, and type as well as exchange current densities are typically deemed proprietary by the manufacturers of this equipment. Therefore, a common practice is to determine these parameters from

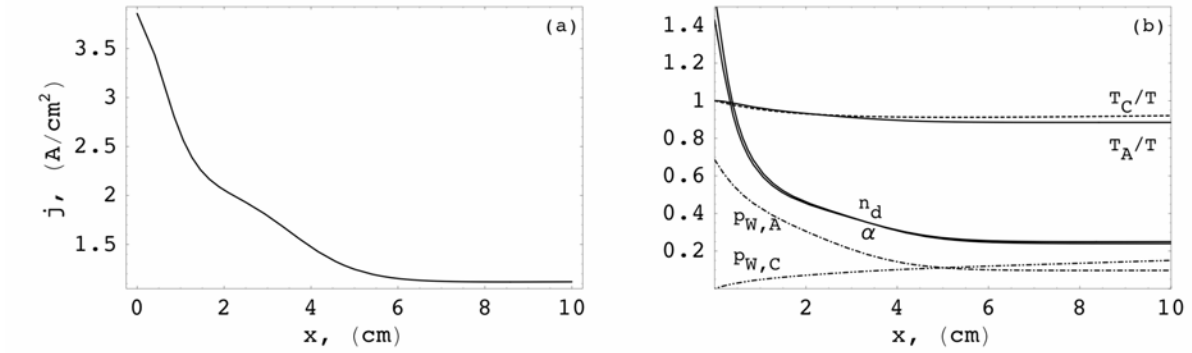


Fig.2. Shows the (a) current density distribution along the channel (10 cm long). In Fig.2 (b) the dimensionless temperature distribution in the anode ($T_A/T$) and cathode ($T_C/T$) is shown; where T is the inlet temperature. Fig.2 (b) also shows the important parameters related to water management, that is the electro-osmotic drag coefficient ($n_d$, dimensionless) and the net water transfer coefficient (alpha, dimensionless).

the open literature. Unfortunately, for the case of both the anode and cathode exchange current densities the range of values varies dramatically from author to author due to the various operating conditions, cell construction, and stack configurations. Typical values for the anode current density, which is the dominate factor in determining the activation overpotential, range from $10^{-7}$ to $10^{-12}$ A $cm^{-2}$.

A nonlinear curve-fitting method is used to determine the exchange current density and conductivity from the experimental current-voltage curve. This approach eliminates the need of seeking this information from the open literature. In addition, the method provides an accurate representation of the cell potential that can be used for integration with a system model where only the performance (IV) characteristics of the FC/electrolyzer models are needed. Highlights of the modeling effort include:

- Experimental IV-characteristics were determined by a commercial electrolyzer at the NREL's hydrogen test facility.
- The experimental information was then used to determine the electrodes exchange current density ($j_A$,o and $j_C$,o) and electrolyte conductivity (sigma) (Fig. 3).
- A non-linear curve-fitting technique was used to determine $j_A$,o, $j_C$,o and sigma.
- The resulting expression (see Fig. 3) can be regarded as an accurate-empirical model easy to implement into a system model.
- The same procedure was repeated at different temperatures and a relation for both the exchange current density as function of temperature was determined (Fig. 4).

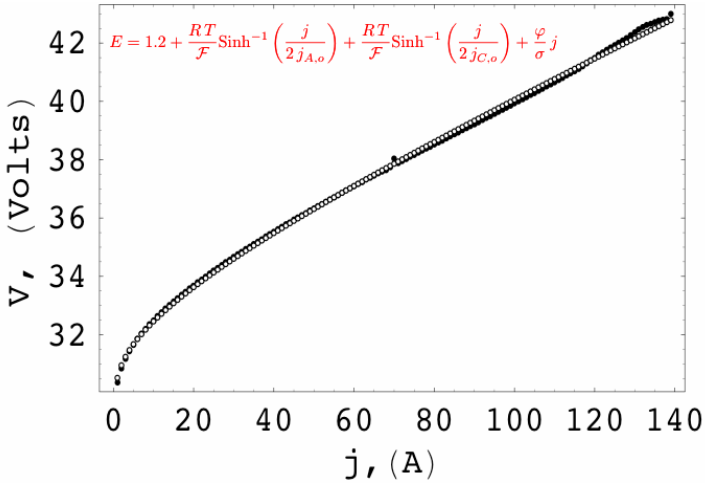


Fig. 3 shows the experimental IV-characteristics (solid dots) and the approximated curve (empty dots). The approximated values for the exchange current density (cathode and anode) and the conductivity are: $j_C$,o=1.65x$10^{-8}$ A/sq.cm, $j_A$,o=0.09 A/$cm^2$ and sigma=0.075 $Ohms^{-1}$ $cm^{-1}$

**Integration with Wind Energy Systems**

The next step in the modeling progression was to integrate the fuel cell and electrolysis models with a wind turbine, diesel engine, and village load. Results from the RPM-SIM modeling are summarized below. Details will be presented in the open literature (see listing at the end of this report).

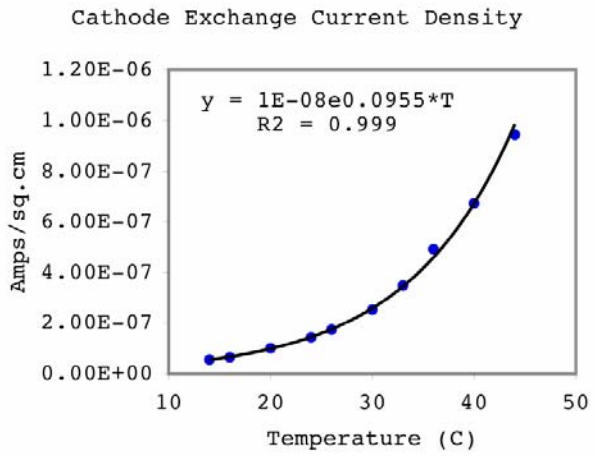


Fig. 4 show the cathode exchange current density as function of the temperature. Starting from a set of experimental IV-characteristics at different temperatures the exchange current density in the cathode was determined by a non-linear curve fitting technique. An expression for the exchange current density, as a function of temperature, is derived from the experimental data.

As the initial step in creating a power system capable of simulating renewable hydrogen generation in an effort to increase wind energy's dispatchability, models for both a PEM electrolyzer and PEM fuel cell were created. RPM-Sim is a set of modeling modules designed for simulating distributed power systems and is compiled in the dynamic mathematical simulation software VisSim.

The electrolyzer model is used to predict the voltage-current characteristics of a 5 kW PEM electrolyzer based on operating temperature and pressure. Energy efficiency, activation and ohmic losses, and hydrogen production are also calculated using the model. The hydrogen production value is particularly useful for determining the amount of hydrogen is supplied to the hydrogen storage module (to be developed).

The fuel cell model is based on the empirical model developed by Yamada and Morimoto of Toyota's Fuel Cell Division. This model solves the equations used by Nguyen and White using the finite difference method to develop an empirical model for a PEM fuel cell based on humidity, operating temperature, and oxygen concentration. This single cell model is implemented in VisSim and scaled to approximate a 50 cell stack. This stack produces an open-circuit voltage of 46 V and is limited to producing a maximum of 6 kW, simulating a commercial PEM fuel cell stack. Fuel cell control is accomplished by limiting the requested power from the DC-AC inverter.

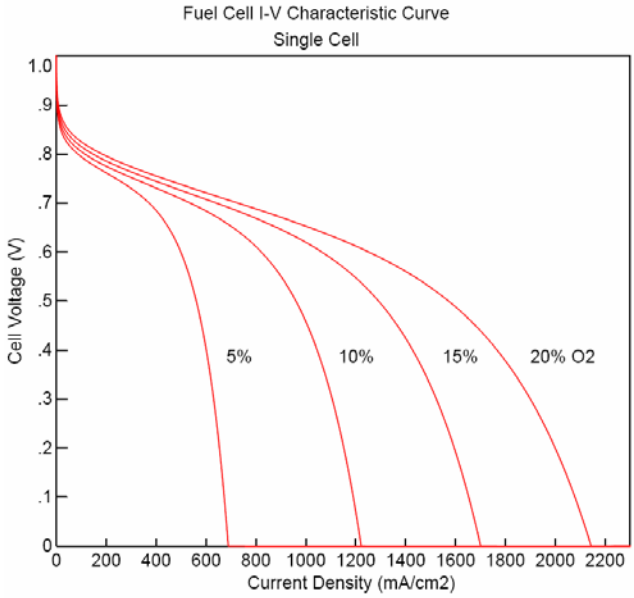


Figure 5: Single cell PEM fuel cell I-V characteristics with varying oxygen concentration

For the case study discussed here (figures 5-13), a fuel cell array is constructed using five fuel cell stacks placed in series. This has the effect of multiplying the single stack voltage by five, ensuring the inverter has sufficient

voltage to operate properly over the range of the fuel cell operation. In this case study, a 75 kW constant load is supplied by a 200 kW diesel generator as the main power source. The 30 kW fuel cell array is told to come online at 3 seconds and supplies 25 kW of power, offsetting diesel fuel usage. At 6 seconds, as the 15 kW wind turbine comes online, it causes a voltage and frequency disturbance as expected with an isolated or weak grid. Once the turbine is producing power, the system returns to steady-state. Both the fuel cell and wind turbine are offsetting fuel consumption by using renewable energy.

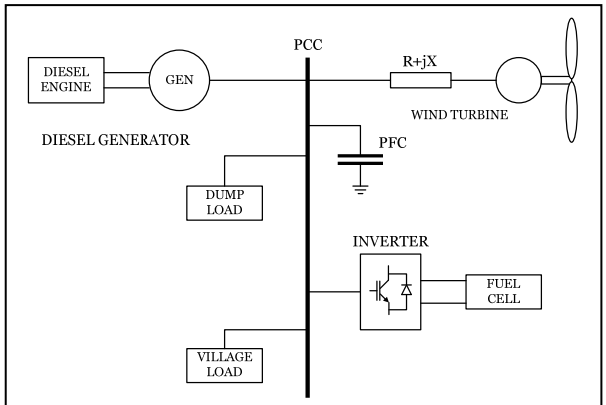

Figure 6. Model configuration

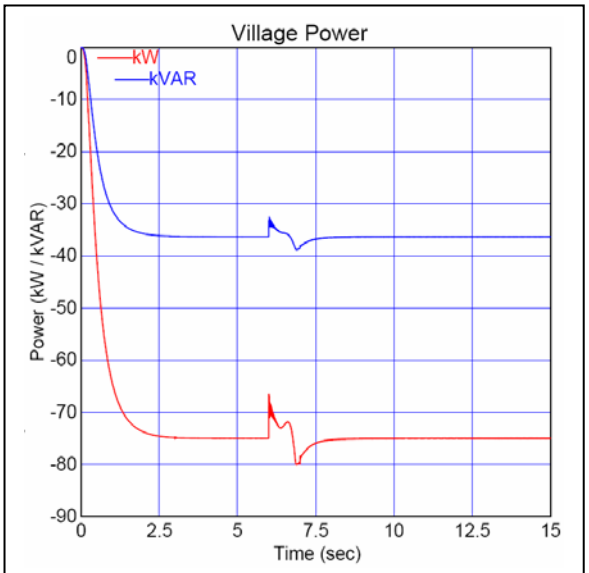

Figure 7. Village load power consumption

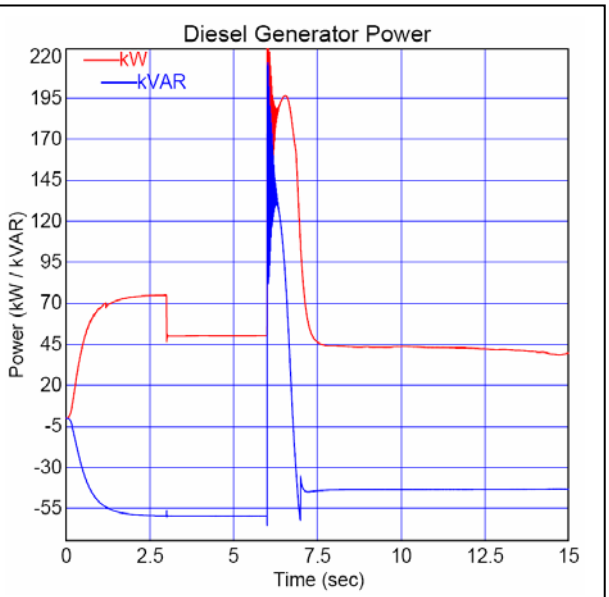

Figure 8. Diesel generator power output

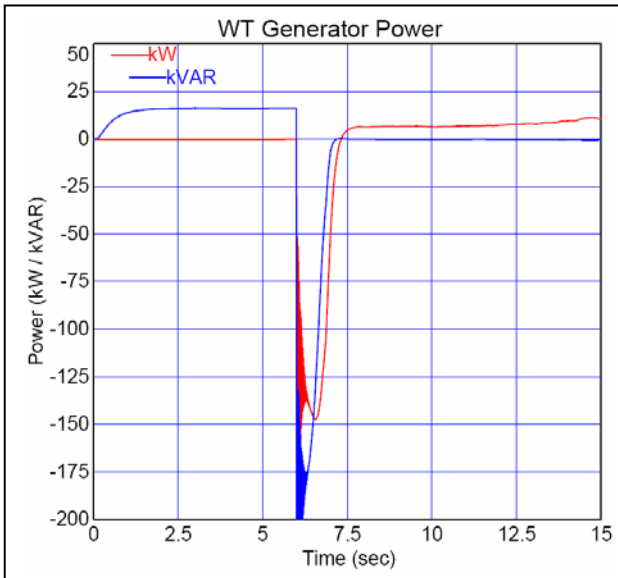

Figuire 9. Wind turbine power consumption and production

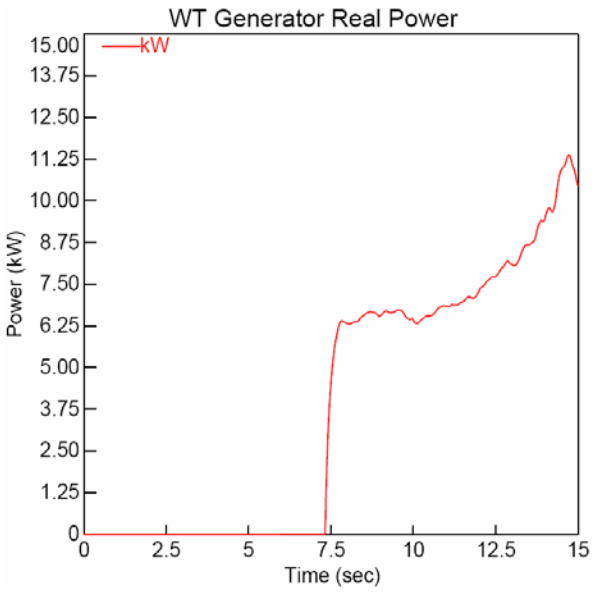


Figure 10. Wind turbine generator real power output

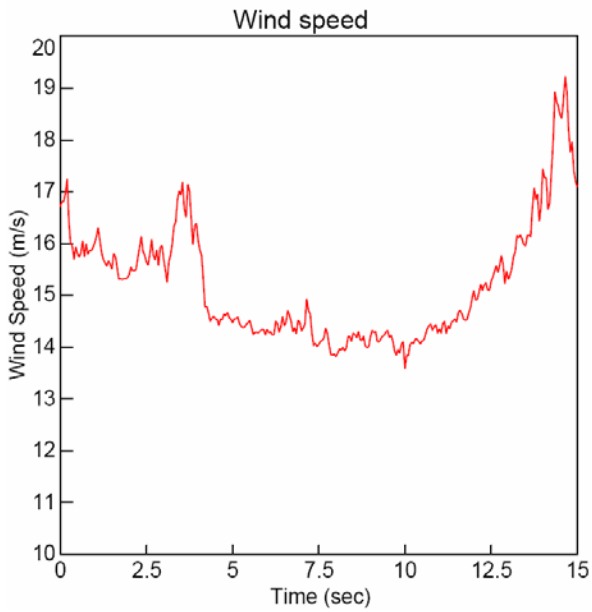


Figure 11 Wind speed for simulation

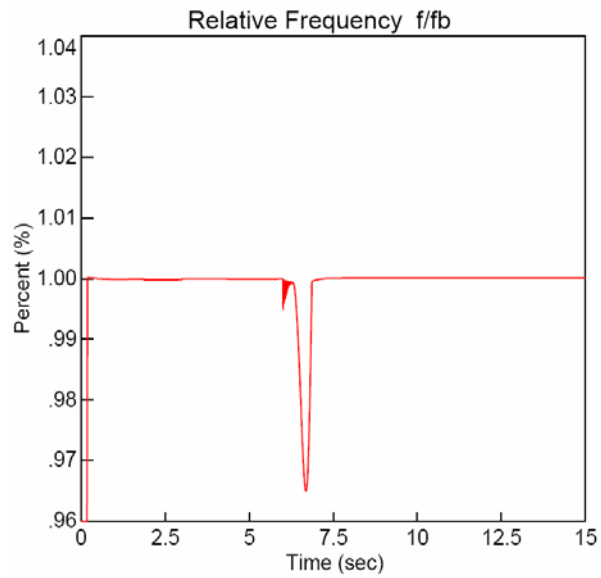


Figure 12. Actual system frequency divided by base frequency shows system frequency accuracy

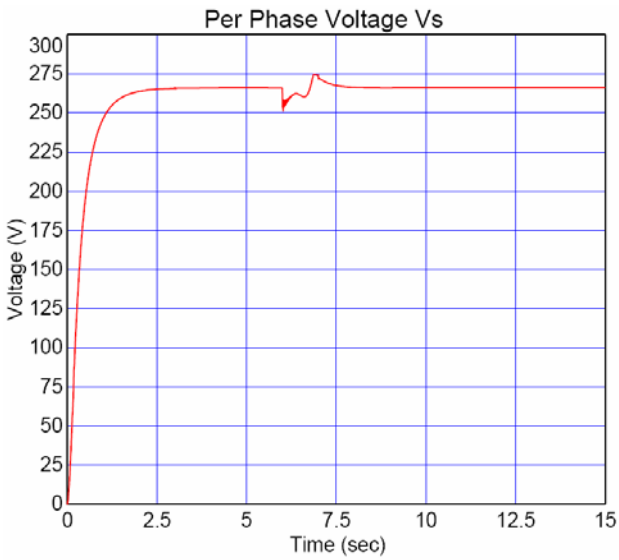


Figure 13. Voltage per phase in system

**Future Work**

Work in this area continues under separate funding from the Department of Energy and the National Science Foundation. Specific activities that are currently underway include:

- Implementing Fuzzy Logic control of the fuel cell to regulate power output under
- variable loading conditions.
- Integration of a fuel cell based system with ultracapacitors as temporary energy storage to cover the temporary energy shortfalls.

- Integration of a fuel cell based system with ultracapacitors to compensate for slow fuel
- cell response to sudden changes in the system demand.
- Development of circuit models of fuel cells and electrolyzers using EIS to study the dynamic response of fuel cells and electrloyzers under various loading conditions.
- Verification of the dynamic response of the fuel cell and electrolyzer from circuit models with the actual dynamic response measurements of the two devices.

2. *Fundamental information on the design and integration of a variable speed wind turbine to electrolysis stack power electronics controller for the production of hydrogen; including wind and electrolyzer power and control systems, direct wind to electrolyzer DC bus power interface, electrolyzer sub-systems when coupled with intermittent power sources (wind, solar, etc.), and the long-term system reliability, availability, and efficiency.*

Work was initiated at NREL to understand and develop a system that could be used to study the important system parameters impacting the performance of a PEM electrolysis system at the stack level. The knowledge gained from NREL was use to construct an experimental electrolysis facility at UND built around a Proton Energy Hogen 40 stack. Constructing the facility from individual components allows UND researchers to conduct a more detailed characterization of the PEM stack performance without all of the ancillary devices present in the HOGEN 40 that was used at NREL. Detailed characterization and efficiency analysis was performed on the individual PEM stack. Further research, based upon input from NREL and Proton Energy Systems utilized Electrochemical Impedance Spectroscopy to generate Equivalent Circuit Models of electrolysis stacks. These models when compared with cell level models resulted in significantly improved tools. Other work included EIS studies on our Ballard Fuel Cell, and development of a new hydrogen drying technique. Results from this work is summarized below, and presented in detail in the various publications presented at the end of this report.

**Development of an Electrolysis Test System at NREL**

NREL's National Wind Technology Center (NWTC) hosted one of UND's Doctoral candidates from May 2003 through January 2004, May 2004 through September 2004, and May 2005 through July 2005. The primary focus was to complete installation and testing on a hydrogen test facility (HTF). The student worked with the NREL team to specify hardware, sensors, and software and assisted in the retrofit of an existing container at the NWTC into one capable of testing hydrogen devices. A major part of this effort was installation and testing of a 7kW proton exchange membrane (PEM) electrolyzer (HOGEN 40RE) manufactured by Proton Energy Systems. The unit was fitted with current, voltage, power, temperature, flow, and pressure sensors to monitor its performance.

Initial testing at NREL focused on establishing a baseline of performance by running the system in its intended modes of operation (constant voltage and current from on-grid electricity). Next, computer generated signals allowed the programmable power supplies to take over the job of powering the PEM stack. Complex (AC+DC) varying frequency and magnitude sinusoidal waveforms (simulating the variable output from wind turbines) are presented to the stack to determine its frequency response. Step waveforms were also generated to determine the response. Results were reported in an NREL document and an ASME paper by Harrison (see bibliography for citation).

## UND’s Renewable Hydrogen Production Research Facility

The UND the team developed a system to extend and compliment the testing being conducted at NREL. Based on the student’s experience at NREL, an experimental electrolysis facility was built around a Proton Energy Hogen 40 stack. Constructing the facility from individual components allows UND

researchers to conduct more detailed characterizations of PEM stack performance without all of the ancillary devices present in the HOGEN 40 that was used at NREL. Detailed characterization and efficiency work has been performed using this system.

Figure 14. UND $H_2$ test facility.

The renewable hydrogen production test facility at the UND (figure 14) consists of a 6 kW PEM electrolyzer system with specially designed control system and two 1.2 kW PEM fuel cells. The system is designed for PEM electrolysis hydrogen production allowing advanced control and monitoring over operating temperature, hydrogen system pressure, water resistivity, water flow, stack current and safety. Along with the temperature, pressure and current-voltage sensors, the main components of the system are a 6 kW PEM electrolyzer stack, hydrogen-water phase separator, two 6 kW Xantrex DC power supplies which are capable to deliver up to 200 A to the electrolyzer, a temperature controlled water loop, a two-tube desiccant drying system and a back pressure regulator to control the operating pressure. Water quality is maintained above defined 1MΩ-cm using mixed bed resins and carbon filters. A temperature control unit (chiller) controls the inlet DI water temperature thereby providing control of the operating temperature of electrolyzer. This system is designed to allow higher temperature testing by maintaining DI water temperature with the chiller and a heater provided in oxygen-water phase separator. Figure 15 shows the overall PEM electrolysis system. Renewable generated DC power is simulated using power electronics packages. A 5.2 kW programmable DC load bank is used for fuel cell studies. A Solartron frequency response analyzer, 1250A with frequency range from 10μHz to 65kHz is used for electrochemical impedance spectroscopy (EIS) studies of both fuel cell and electrolyzer at the cell and stack level.

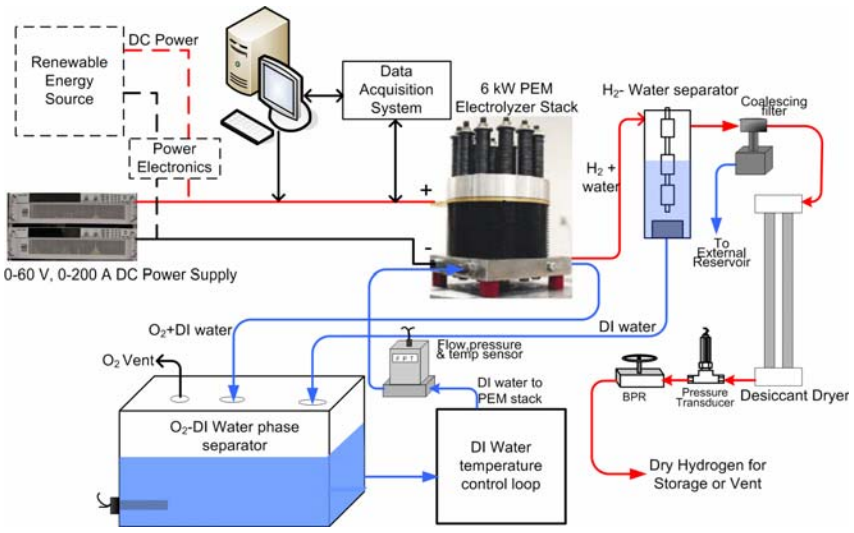

Figure 15. Schematic of UND's electrolysis test system

The developmental work currently being performed at UND in this area is carried out primarily by the Departments of Chemical and Electrical Engineering, with support from the Chemistry Department. This is an advantage of a smaller university like UND – collaboration across departments is natural. Although we involve students at all levels, we currently rely on PhD students to perform the bulk of our research. This gives us the capability to explore research questions in great depth. We are application oriented with a great depth in theoretical concepts. The experimental component of our program provides the data and capability to verify the models that we are developing. In addition, we view applications from the system level, rather than the component level. Having a strong modelling and experimental component, coupled with an eye toward overall system level efficiency has helped us keep our research meaningful.

**Dew Point Control**

Proton Energy Systems (PES) manufactures PEM electrolysis equipment incorporating an adsorbtion drying system to remove water vapor from the hydrogen product gas. The PES line of electrolyzers utilizes a two-tube desiccant-drying system to achieve a dew point of -65 °C, or less than 5 parts per million (ppm) water vapor, in the hydrogen product gas (99.9995% pure hydrogen). The two-tube desiccant system uses one tube at a time to dry the hydrogen from the PEM stack. At full operating current an orifice at the top of the drying assembly diverts roughly 10% of the dried hydrogen down the opposite tube to remove the adsorbate from the adsorbent. After a predetermined amount of time, solenoid valves divert the hydrogen to the opposite tube and the same orifice is used to regenerate the adsorbed tube with the dry hydrogen.

An alternative method to reduce and control the dew point of the hydrogen gas has been developed (see figure 17). Thermoelectric coolers (TECs) are used to cool saturated hydrogen gas as it travels through a large-surface-area cold plate, allowing the water vapor to condense in Stage 1 and sublime in Stage 2. Two cooling stages are presented to condense and sublimate water vapor from the hydrogen stream in an effort to achieve a dew point below 0 °C. The goal of the first TEC stage cold plate assembly is to reduce the dew point from approximately 35 °C to near 0 °C. Stage 1 will allow the parallel connected TECs in the second stage to run longer at temperatures well below 0 °C. Pressure sensors monitor Stage 2 and switch between the parallel connected cold plates when frozen water begins to restrict hydrogen flow within the finned cold plate. By reversing the polarity of the TEC power supply, the cold plate will be heated, causing the ice buildup to melt and be collected downstream by a coalescing filter. Figure 18 shows the detailed components of a TEC module and the DC power supply wired to cool the cold plate on top.

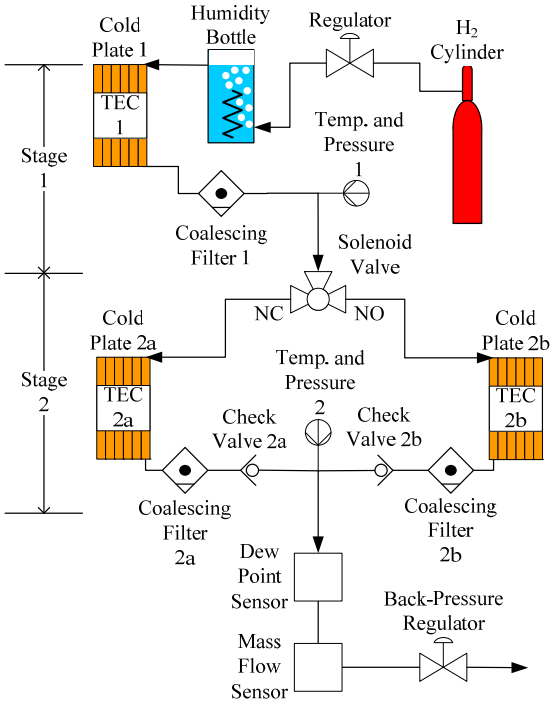

Figure 17 Experimental system design.

In order to maximize the benefits of a TEC, the heat must be removed from the hot side using a heat sink. In addition to removing the heat from the object being cooled, the heat of the TEC operation (waste heat) must also be removed. These two sources of heat require a high density of heat to be removed from the TEC surface. Using a conventional air-cooled heat sink is an option, but in order to dissipate a large number of watts (e.g., 100 W) at typical room temperatures, the heat sink and fan become large. Water-cooled heat sinks offer compact sizing, superior performance over air-cooled heat sinks, and are nearly silent when operating. For this reason and the readily available water source inherent to an electrolyzer system, a water-cooled heat sink was selected for this design.

In the system designed by the UND team, hydrogen gas leaving a PEM stack is assumed to be fully saturated with water vapor at temperatures above ambient. To simulate the output from a PEM stack, this

experimental design bubbles dry hydrogen gas from a pressure-regulated storage cylinder through a humidifier to fully saturate the gas. An input regulator downstream from the high-pressure $H_2$ cylinder and a back-pressure regulator at the output of the system will be adjusted to achieve the desired hydrogen flow rate. The humidity bottle contains a submersed heater coil to control the exit gas dew point. The entire system incorporates three cold plate assemblies (CPAs) in two stages. For this proof-of-concept testing, an operating pressure of 345 kPa (50 psig), flow rate of 1 $Nm^3\ hr^{-1}$, and saturated hydrogen gas around 35 °C will be presented to the TEC-based drying system.

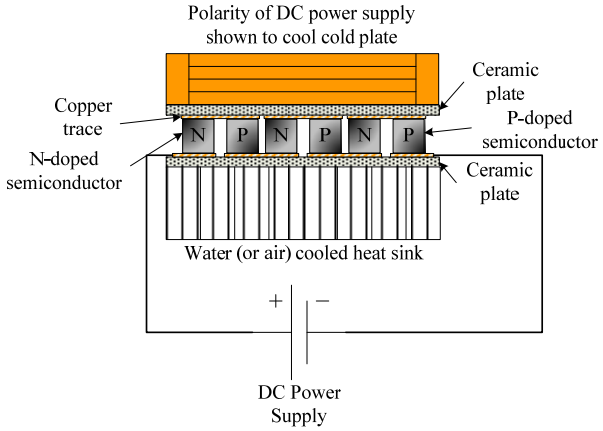


Figure 18 Typical thermoelectric device configured to cool the cold plate on top.

The CPA consists of a high-surface-area cold plate, TEC and water-cooled heat sink. In the system shown in figure 17 two stages of cooling are used to reduce and control the dew point below 0 °C. Stage 1 has saturated hydrogen gas as its input and uses a single 36 W TEC module to reduce the dew point to slightly above 0 °C. Stage 2 requires two CPAs in parallel to achieve dew points below the freezing point. Coalescing filters are located immediately downstream of each CPA to remove liquid water from the process. Temperature, pressure, dew point and mass flow sensors will monitor the performance of the system.

Figure 19 shows the detailed configuration of the CPA. Water-cooled heat sinks were chosen based on their exceptional ability to dissipate the high density of heat pumped/generated by TEC devices and the readily available source of water and DC electricity in an electrolysis system. This approach seemed to be a natural selection for dissipating the sensible and latent heat required to condense and sublime water vapor from the hydrogen product and remove the waste heat of the TECs.

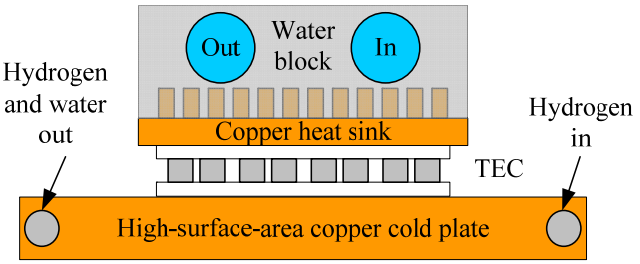


Figure 19. Detailed CPA showing the cold plate, TEC and water cooled sink

The two-stage cold plate and thermoelectric design may contain other operational benefits depending on the application for which the hydrogen is being produced. The TEC design can obtain dew point control with closed-loop feedback of the TEC temperature in Stage 2 to obtain the desired dew point to match the application. The TEC design consumes roughly 5 kWh per day, while the desiccant system loses roughly 7 kWh of hydrogen per day to maintain the desiccant. Further testing of the device is ongoing to fully characterize the benefits of this device

**EIS of 1.2 kW Fuel cell**

Preliminary EIS work investigated the performance of a 1.2 kW PEM fuel cell stack using a frequency response analyzer on temporary loan from Gamry Instruments. The application of EIS to working fuel cells stacks is a departure from its traditional applications and as a result, measurement techniques are modified to acquire meaningful data. When EIS is used to study cells in corrosion and coatings, the

activity of interest is primarily an electrochemical reaction and charge transport. However, in a working fuel cell stack, these activities are constantly interacting with load and control algorithms. It is important therefore to be able to isolate spectral data behavior that is associated with each of these mechanisms.

Our first study investigated three parameters that could affect the impedance spectrum of a working PEM fuel stack. These are namely the test signal amplitude, the fuel cell control algorithm, and the test cell position in stack.

***Test Signal Amplitude:*** Typical EIS investigations study steady-state processes, with the amplitude of the test signal chosen small enough to avoid excessive disturbance. These studies are good for studying the membrane properties. In addition to the classical studies, we investigated the response of the PEM fuel cell in the presence of large amplitude test signals, up to and including amplitudes higher than the direct current drawn from the fuel cell, requiring a current reversal.

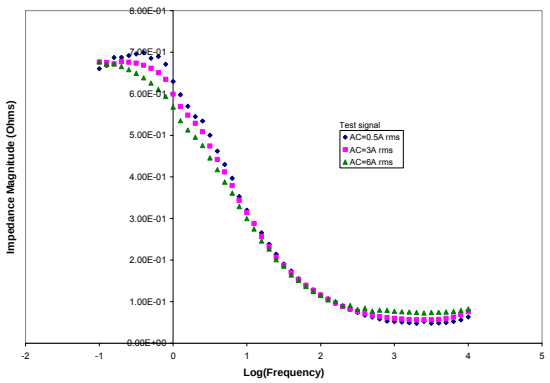


Figure 20: Magnitude plot of impedance spectrum of a 1.2 kW PEM fuel cell stack with electronic load drawing 5A direct current with EIS signals of various currents superimposed.

Results, presented in figure 20, show that at both high and low frequencies the size of the amplitude of the test signal resulted in noticeable variation in the impedance of the fuel cell. It was also observed that choosing test signal amplitude larger than the direct current loading of the fuel cell did not result in impedance that was completely different from the others. Results from these ongoing studies are being used to develop equivalent circuit models for analysis of voltage stability, short circuit conditions, transient responses, power quality, protection schemes, and optimizing dynamic operational performance.

***Control Algorithm:*** Several control algorithms are employed in fuel cell systems for protection and to enhance the quality of power generated. Previous work indicated that the cathode purge, which restores the decaying voltage due to the accumulation of water and nitrogen in the cathode channels, could impact EIS data. An investigation of this process showed that for the Ballard Nexa™, the cathode purge results in a voltage change of 0.08 V per cell within the load range studied. This results in a sudden change of 9% in voltage when the fuel cell is not loaded. If the fuel cell is loaded this percentage increases. The shape of the decay curve changes with the loading on the fuel cell (see figure 21). If the voltage change caused by the test signal is comparable with the purge voltage change (0.08A) the interaction results in noisy impedance data. This experience demonstrates the inherent noise present in EIS when using an integrated system with a built in control. To avoid this, it is necessary to decouple the stack from the vendor supplied integrated control system, and/or to carefully chose amplitudes to minimize the signal to noise ratio. The PEM electrolysis system currently used in the UND studies has been designed to remove the vendor imposed control.

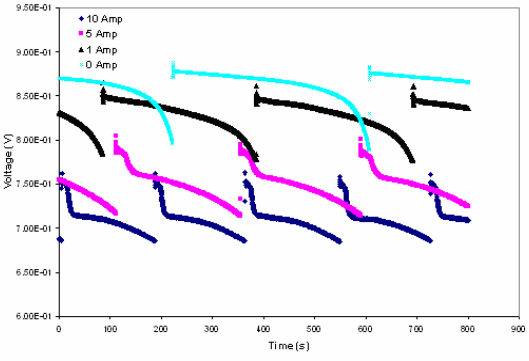


Figure 21. Decaying voltage of a 1.2W fuel cell loaded with parasitic devices and electronic load drawing 0, 1, 5& 10 amps

***Test Cell Position:*** It is tempting to assume that all cells in a stack behave alike. This simplifies modeling efforts, allowing single cell models to be utilized to represent stack performance. However, based upon transport and other considerations that occur at the stack level, we expect some variance. Is this variance significant, and does it warrant independent studies? For the Ballard Nexa™ PEM fuel cell, significant variation occurs as a function of cell position. Ten cells were taken at different locations in the stack and the impedance data measured. It was found in the Nyquist and Bode magnitude plots that the membrane resistances were unchanged. However, the activation resistance had changed. The Nyquist plot for this phenomenon is shown in figure 22. Other performance characteristics such as ionic conductivity, activation resistance and current distribution changes per cell can be compared between the cell and stack level. Identifying and understanding these differences will provide designers information to help identify which design aspects can result in the most significant improvement. Improving membrane and electrode porosity, developing better catalysts and improving channel design will minimize losses and improve efficiency.

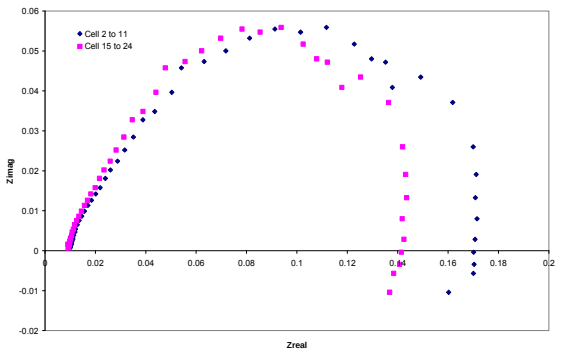


Figure 22 : A comparison of the Nyquist plot of a group of the cells taken at different locations in the 1.2 kW PEM fuel cells

**Additional EIS Studies of PEM Fuel Cells**

Ac impedance studies were performed of a commercially available proton exchange membrane (PEM) fuel cell at various operation loads using a Ballard 1.2 kW Nexa™ system. The PEM fuel cell stack was operated using room air and pure hydrogen (99.995%) to study the stack, groups of cells and single cell behavior at various loads. The electrochemical impedance analysis shows the low frequency inductive effects and mass transport losses due to liquid water accumulation at high current densities. Effects of artifacts related to experimental set up on high frequency and low frequency loop intercept was also examined. We felt this study was important since most of the EIS studies reported in the literature are focused on single cell [i,ii,iii,iv], and those performed on fuel cell stacks [v,vii] do not take into account the effect of control systems integrated with the fuel cell stack on its behavior.

The impedance data was collected using Solartron 1250A frequency response analyzer (FRA) and Chroma 63203 programmable DC electronic load. The Solartron 1250A FRA has a frequency range from 10μHz to 65 kHz. The Chroma DC electronic load has a frequency range up to 20 kHz. The impedance spectrum was recorded by sweeping frequencies over the range of 20 kHz to 50 mHz with 10 points per decade. The EIS experiments were carried out in galvanostatic mode which is usual mode of fuel cell operation and current control is easier than voltage control with commercial electronic loads [vi,vii]. The EIS measurements for group of cells at different locations in stack were carried out by measuring voltage directly across the group of cells and the current was measured at the electronic load. Before each measurement the fuel cell was operated for at least one hour at a particular current.

Selection of the AC signal amplitude is an important issue in fuel cell EIS experiments to ensure good impedance spectra is obtained. For accurate EIS measurements the perturbation signal has to be sufficiently small in the ranges of 5-10 mV peak to peak [viii]. However, with small AC signals FRA can not distinguish between noise and response. For this study, tests were conducted to obtain impedance spectra at AC amplitudes of 1%- 5%, 7.5%, 10% and 15% of DC. Based on results an AC signal of 10 % of DC resulted in good impedance spectra and was used for further testing. Also as a part of the initial characterization, the effects of external wire resistance and connections on impedance spectra are

explored. The effect of self inductance on the impedance spectra at high frequency loop of each wire connecting the system was explored to make recommendations on proper installation and use.

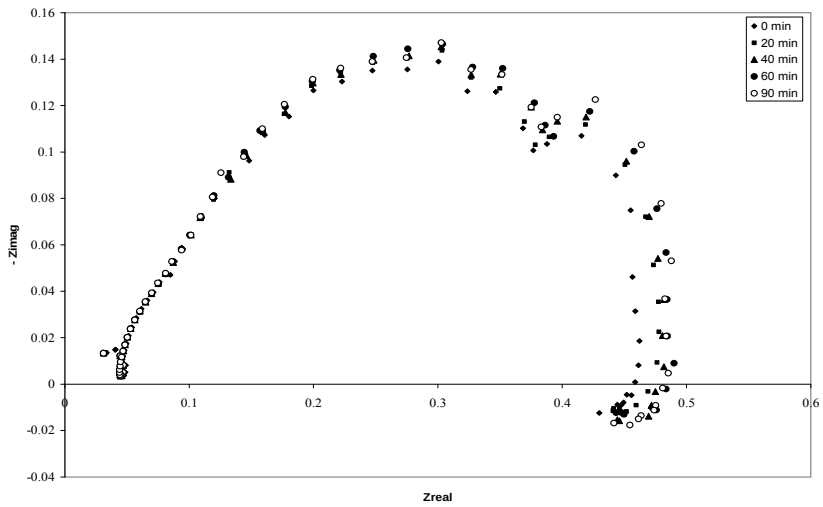

Figure 23: Impedance data recorded at different stack run time for 10 Adc with ac signal of 10 % of dc.

The system under study must be at steady state throughout the EIS measurement [4]. EIS measurements were taken at 1 min, 20 min, 40 min, 60 min and 90 min of stack run time, with each set of measurements taking approximately 11 min. The stack was running at DC test current continuously in-between these tests. As can be seen in figure 23, the impedance spectra gets bigger as time of start of the test increases. The difference between the impedance data at low frequency taken at the beginning (1 min) and after 60 min can clearly be seen in figure 23, and stresses the importance of taking data at steady state to avoid misinterpretation of the data. The same results were obtained for various current levels. Our work was performed after the fuel cell stack has to run for at least one hour.

The impedance of the 47 MEAs stack was measured using FRA and DC electronic load at different current levels and Nyquist and Bode plots developed (figures 23 and 24). The typical impedance spectra in Nyquist plot show three semicircle loops. The high frequency loop starts from 20 kHz to 1 kHz and corresponds to anode activation losses while the low frequency loop starts from 1 kHz to 0.1 Hz and corresponds to cathode activation losses. At high currents a third loop can be observed at low frequency which represents the mass transport losses. At low currents the two characteristics loops are seen in figure 24 for currents 1 Adc - 4 Adc. The third loop starts appearing at 5A dc and more. The bigger low frequency loop (1 kHz to 0.05 Hz), shows the cathode activation losses are higher than the anode activation losses and can be attributed to slow kinetics of the oxygen reduction reaction (ORR) at the cathode. Hydrogen electrode kinetics are faster

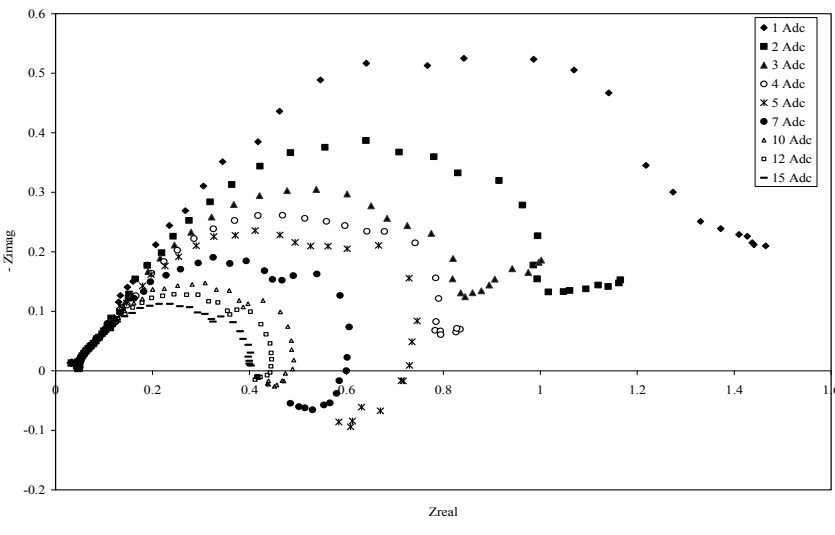

Figure 24: Current dependence of Nyquist plot for the current range 1 Adc to 15 Adc with ac signal amplitude of 10% of dc

than oxygen electrode. The changing behavior of the low frequency loop as current increases is also related to the double layer capacitance of the electrode combined with charge transfer resistance of the ORR. The diameter of this loop is determined by charge transfer resistance. Dependence of charge transfer resistance on electrode potential is given by Tafel equation [ix,x]. As shown in figure 24, the bigger loop (low frequency loop) shrinks at high currents and third loop representing mass transport losses appears at 5 A dc and more. The inductive effects also appear at high currents. The possible reason suggested by Makharia et al [xi] is the side reaction and intermediates involved in fuel cell reaction. However, this low frequency inductive behavior can also be attributed to time required to make measurements at low frequency, or, nonstationary behavior. An impedance model developed by Roy et al[xii] to account for the reaction mechanism that may be responsible for the inductive response at low frequencies proposes the formation of hydrogen peroxide as an intermediate in a two step ORR.

The polarization resistance at 1 Hz had changed from 1 Ω at 1 Adc to 0.38 Ω at 15 Adc as can be seen from figure 25. The impedance modulus matched closely at high frequencies and started deviating approximately at 10 Hz. The impedance modulus showed a continues increase from 1 Adc to 4 Adc. However, change in the shape of impedance modulus plot at lower frequencies (< 2 Hz) observed from 5 Adc and higher. After reaching the peak value the impedance modulus started decreasing which corresponds to inductive effect observed in the Nyquist plot (figure 24). A close observation of Bode plot showed a small dip in impedance modulus in the frequency range 2 Hz to 0.3 Hz before it reached the peak. This nature of the plot represents the mass transport loop in the corresponding Nyquist plot.

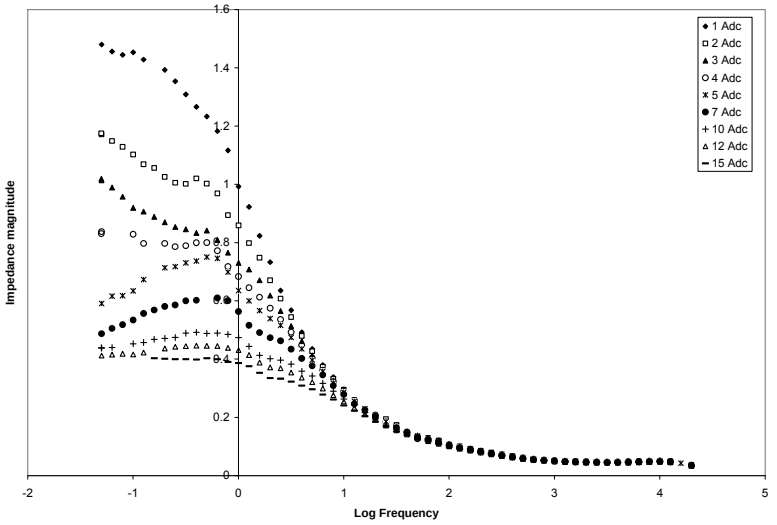


Figure 25: Bode plot for current range 1Adc to 15 Adc with ac signal amplitude 10% of dc

The fuel cell runs at higher current densities to achieve high power. However, at high current densities the mass transport losses become more significant. Figure 26 shows the impedance data at high currents (20 Adc-40 Adc). The third loop at low frequency gets bigger as current increases. The inductive nature of these loops also increases at higher currents. The increased mass transport losses at higher currents can be reduced by modifying the operating conditions; such as operating at a higher reactant flow rate [xiii]. H. Young et al [xiv] have operated a fuel cell more than 20 times the stoichometric flow rate.

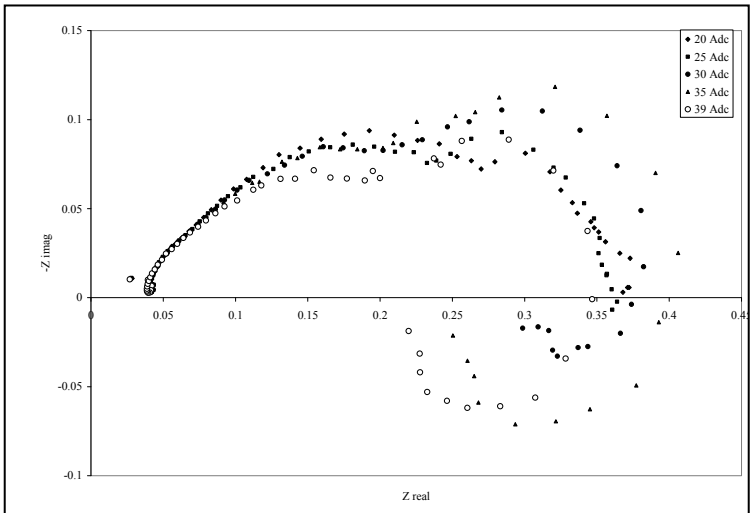


Figure 26: Current dependence of Nyquist plot for current rage 20 Adc to 39 Adc with ac signal amplitude of 10% of dc

In case of the commercial fuel cell used for this study, the oxidant air flow rate increases proportional with the current, therefore, the increased mass transport losses may not be cause by low oxidant air flow as was the case in other studies.

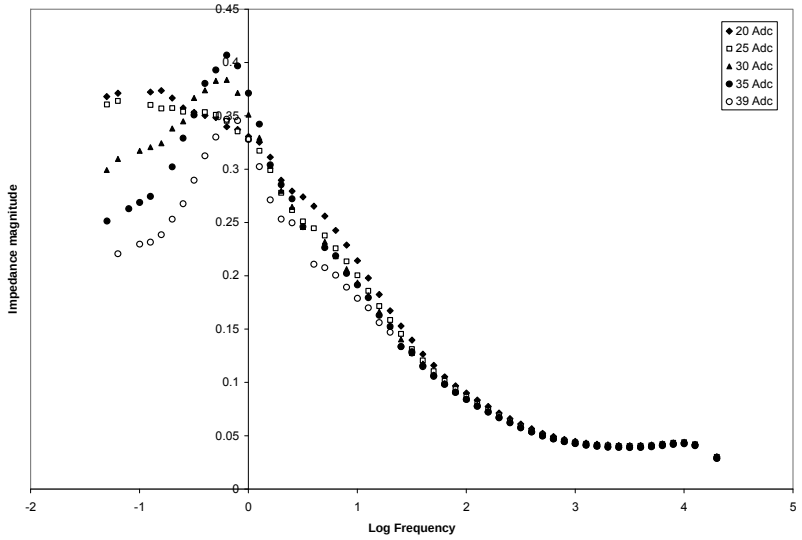

Figure 27: Bode plot for current range 20 Adc to 39 Adc with ac signal amplitude 10% of dc.

As can be seen in figure 27 from the impedance plot, the low frequency arc (3rd loop) becomes more prominent with increasing current. Another explanation for this third low frequency loop is the effect of liquid water formed at the cathode, which affects the transport of oxygen and the hydration effects that limit the water transport in the membrane [xv]. Paganin et al [xvi] attributed this third low frequency arc to the water transport characteristics in the membrane. Water diffusing through the membrane to the anode side increases with the load, but at higher current densities, close to rated current, a significant amount of water reaching the anode is transported back by electro-osmotic drag. The size of the third arc may depend on which one of the diffusion and electro-osmotic drag mechanisms dominate the process at that current density.

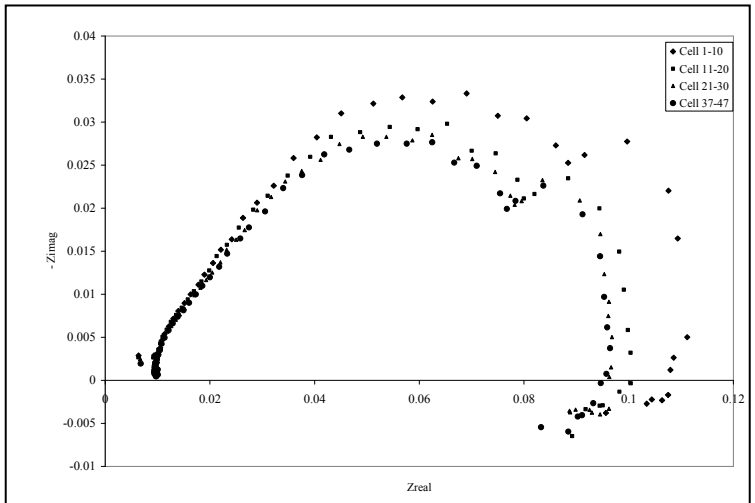

Figure 28: Nyquist plot for group of ten cells at different positions in stack

A group of ten sells were selected starting from the air inlet to investigate the effect of cell positions in the stack on impedance data. The cells were numbered from air inlet side starting from 1. Figure 28 shows the impedance plot for group of 10 cells at different locations. For this investigation 10 A dc load current was used with AC signal amplitude of 10% of dc load current. As can be seen from figure 28 the cells located at the hydrogen inlet have less impedance than cells located at the air inlet side. Not much difference was observed in the high frequency region. At high frequencies the impedance is mainly resistive. However, at low frequencies, changes are observed in both polarization resistance and the capacitance component from the hydrogen inlet to air inlet side cells. The membrane resistance did not change with the cell positions in the stack. Its value was 6.5 mΩ for group of ten cells compared with 30 mΩ for the whole stack. The membrane resistance for each cell from the figure 28 can be estimated as 0.65 mΩ. The membrane resistance values for each cell sumps up closely to the whole stack membrane resistance as should be the case for cells connected in series.

As shown in figure 29, all the selected group of ten cells had the same impedance magnitude at high frequency. The impedance started separating form other groups at 100Hz and continues till 0.05 Hz. At 1 Hz, the impedance modulus of group of cell # 1-10 located at the air inlet side found 17 mΩ more than that of cells # 37-47 located near hydrogen inlet. At high frequencies the impedance modulus matched closely for different group of cells. The deviation at low frequencies increased with the capacitance component of the impedance increased as shown in figure 26. The reason for the change in polarization resistance at low frequencies observed in Nyquist (figure 28) and Bode plot (figure 29) with cell positions in stack is unclear. If a temperature gradient has caused this change then the membrane resistance should also have changed as membrane resistance is a function of temperature. Since no change was observed in the membrane resistance, the polarization resistance change with position may be attributed to non-uniform distribution of current density along the stack.

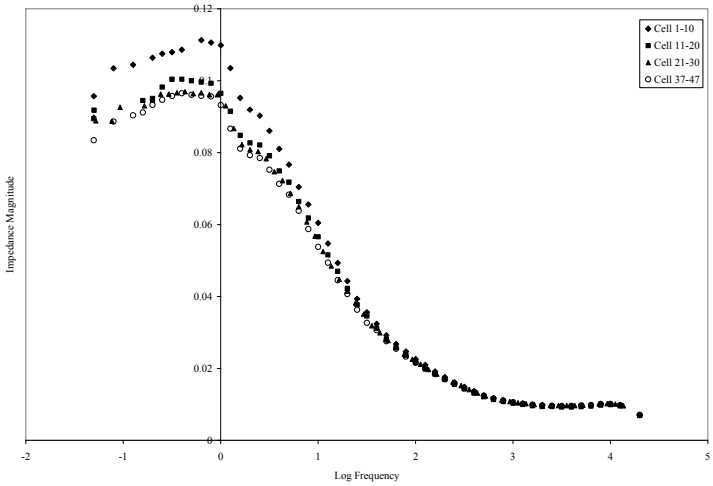

Figure 10: Bode plot for group of ten cells at different positions in stack

To investigate the impedance behavior of cells located at the hydrogen and air inlet, EIS tests were conducted to on group of five cells at each end. Based on the results obtained for the group of ten cells at different positions in stack, the impedance of cell # 1-5 was expected to be higher than cell # 42-47 as shown in figures 30 and 31. The change in polarization resistance from 46 mΩ to 58 mΩ was observed for group of five cells for air inlet and hydrogen inlet side respectively. The non uniform current density distribution may be the cause for this polarization resistance change. The exact reason is unknown at this point.

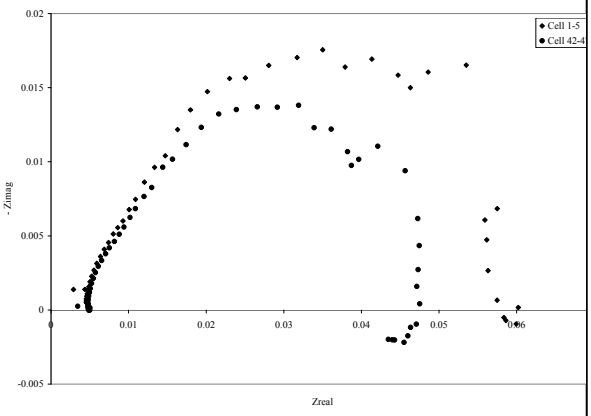

Figure 30: Nyquist plot for group of five cells at either end of fuel cell stack

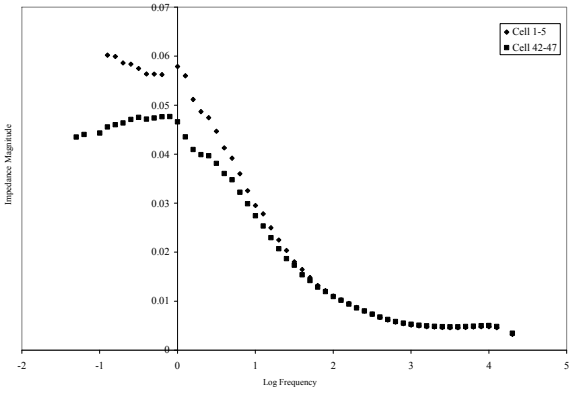

Figure 31: Bode plot for group of five cells at either end of fuel cell stack

## PEM Electrolysis IV Characteristics

The UND PEM electrolysis system is designed to allow experimentation at different operating conditions. Variables including temperature, pressure, stack current and water quality can be precisely controlled and monitored. Early work focused on operating temperature to provide data that can allow peak efficiency to be obtained regardless of operating current. This will be beneficial in variable power sources such as renewable energy. As shown in figure 32, for a given current, voltage drops as temperature increases. This increases stack efficiency as activation and ohmic losses (irreversible potentials) are reduced. At higher temperature the stack produces more hydrogen at a given current.

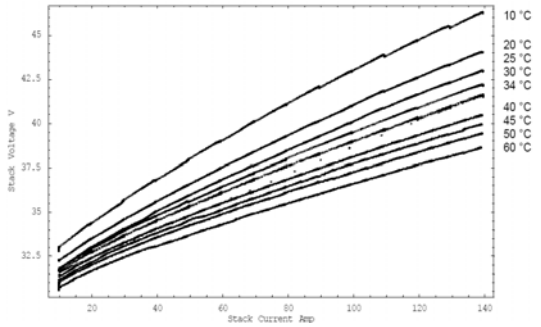


Figure 32: IV characteristic curves at constant cathode pressure (165 psi) at temperature from 10 °C to 60 °C. (all temperatures have +/- 0.4 °C error margin)

### Charge Transfer Coefficient Dependence on Temperature

A study was conducted on the charge transfer coefficient (CTC) of the oxygen electrode (anode) of our PEM electrolyzer stack to determine its temperature dependence. CTC is defined as the fraction of the applied potential energy to an electrochemical reaction that increases the reaction rate. In recent modeling studies of electrolyzer stacks based on electrochemical thermodynamics, CTC has been assumed to be equal to the symmetry factor for the oxygen electrode, defined as the fraction of charge transferred during the activation step of a reaction at an electrode. Its value is typically 0.5 at both the cathode and anode of an electrolyzer. For reactions in which there is only one electron transfer as in the hydrogen electrode of the PEM electrolyzer, the CTC value is numerically equal to the symmetry factor. On the oxygen electrode, however, the CTC has been reported to vary from 0.1 to 0.5, and some authors have reported even higher values up to 0.6. An accurately determined CTC not only predicts the current-voltage characteristics of electrolyzers better, but also gives insight into the reaction mechanisms and the properties of the electrode.

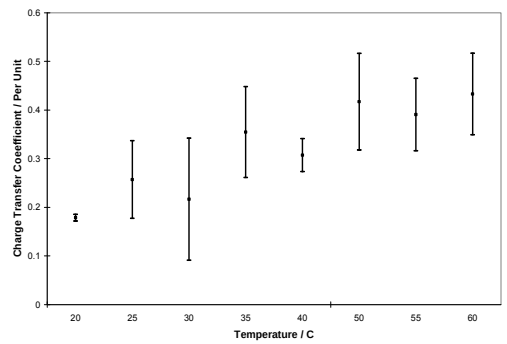


Figure 33: Variation of anode CTC with temperature.

Studies at UND found that variation of CTC from the symmetry factor is significant enough to impact the estimation of the activation overpotential. Figure 33 shows the variation of the anode charge transfer coefficient with temperature. Clearly there is an upward trend with temperature which could be the result of reaction modification or changes in electrode properties with temperature. The behavior of the CTC shows that the better performance observed for the electrolyzer stack at higher temperatures is not solely reliant on the increased membrane conductivity but also depends on the CTC. The upward trend observed in the value of the CTC is an indication that the kinetic characteristics improved as well with temperature.

This study confirmed that CTC at the oxygen electrode of an electrolyzer exhibits more variation than at the hydrogen electrode. If the reports that the CTC is only electrode and reaction dependent are true, then it can be inferred that temperature indirectly affects the CTC by changing the properties of the electrode or the reaction mechanisms or both. Accurate determination of the CTC of PEM stacks is important to take advantage of the increasing body of knowledge on CTC to improve the micro-kinetics of future electrolyzers.

**Electrochemical Compression**

PEM technology can be used to compress hydrogen. Using PEM hydrogen feed at the anode, as shown in figure 34, oxidizes to protons ($H^+$) by the application of a potential difference. These protons transport through the polymer membrane and reduce to hydrogen again at the cathode. The hydrogen being produced by proton reduction in the confined cathode space is compressed and discharged at high pressure. As the polymer membrane is selective for hydrogen, inert gas components can not cross the membrane and thus removed from the compressed gas. Moreover, since the electrochemical compressor does not have any moving parts, it minimizes maintenance. Flexibility in sizing of cells allows this compressor to achieve a high efficiency.

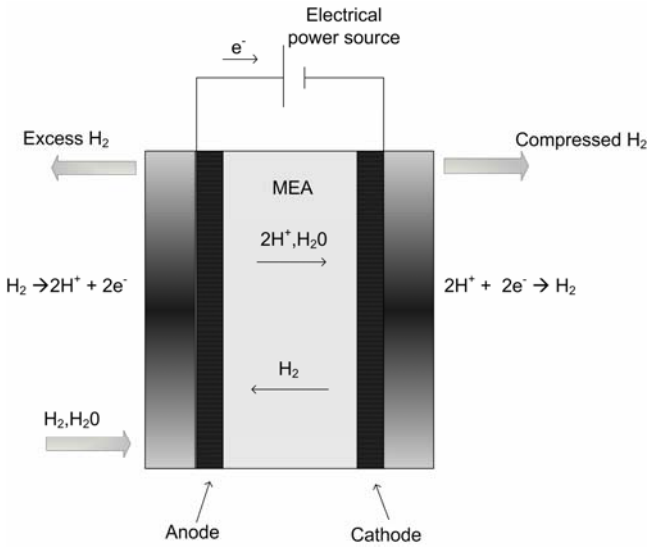

Figure 34. Polymer electrolyte membrane hydrogen compressor

Overpotentials are the irreversibilities that have to be overcome by applied potential to a PEM cell before oxidation and reduction of hydrogen can begin. For a PEM cell working as an electrochemical compressor only activation and ohmic overpotentials are significant as modeled by the Tafel equaiton. Generally, the kinetics of hydrogen electrodes are rapid. But in case of a PEM cell compressor, slightly slower kinetics of the reduction at the cathode can be observed as compared to the oxidation at the anode. Theoretically calculated anode and cathode overpotentials increase with increasing current densities as shown in figure 35. The anode exchange and cathode exchange current densities from literature [xvii, xviii] are used for this modeling work.

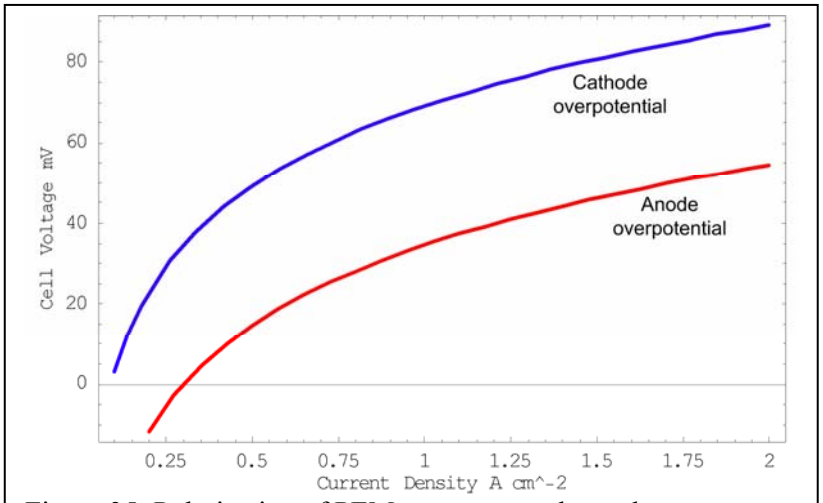

Figure 35: Polarization of PEM compressor electrodes

The constant resistance experienced across the applied voltage to the PEM cell is represented as ohmic overpotential. The magnitude of ohmic loss depends on electrode material, electrolyte material and interface between electrode and electrolyte. Manufacturing processes and techniques are an important factor in keeping this overpotential minimal. Calculated total cell voltage and Nernst potential over a pressure range is shown in figure 36. To simplify modeling work, the anode pressure is assumed to be constant at 1 atm (14.7 psi). The calculations were done at 60°C.

As can be seen from figure 36, the main contributor to cell voltage are ohmic and activation polarizations. Efforts were taken to estimate the contribution of each of these polarizations towards the total cell voltage at various operating current densities. Figure 37 shows these contributions to the total cell voltage. The ohmic voltage almost amounts to the cell voltage.

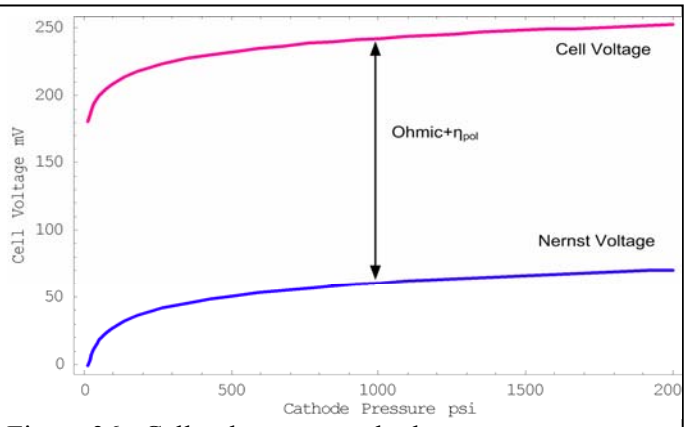

Figure 36: Cell voltage versus hydrogen pressure at the cathode.

In the real situation, the assumption of constant anode pressure can not be true. The high pressure difference across the membrane promotes the back diffusion of molecular hydrogen from cathode to the anode side. The back diffusion rate is also important for efficiency calculations, as the compressor efficiency decreases with increasing back diffusion. The back diffusing hydrogen, which increases the pressure at the anode side, varies with varying cathode pressure and cell temperature and can be measured by the amount of compensating current to keep the anode pressure constant. Efforts to model the contribution of back diffusion are underway.

Cell voltages were calculated at different cathode pressures and plotted as a function of operating current densities to show the relationship between input energy and hydrogen pressure (figure 28). For this calculation the anode pressure is assumed constant at 1 atm (14.7 psi) and the product pressure at the cathode is varied from 250 psi to 2000 psi.

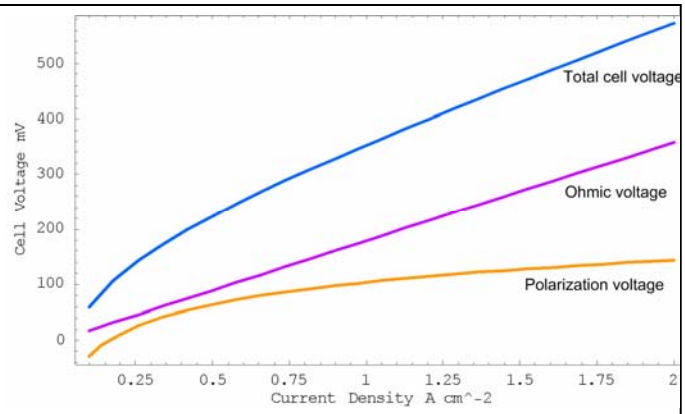

Figure 37: I-V characteristics of PEM cell compressor.

As expected, higher cell voltage at higher pressure shows more energy requirement to compress hydrogen to an elevated pressure. In practical situations, the voltage differences are small at low current densities and more significant at higher current densities. Also the measured voltage can be greater than that calculated by equations because of increased resistance of the cell. Higher pressure difference between anode and cathode causes expansion and contraction of the material inside the cell which results in increase of contact resistance and therefore leads to higher voltages.

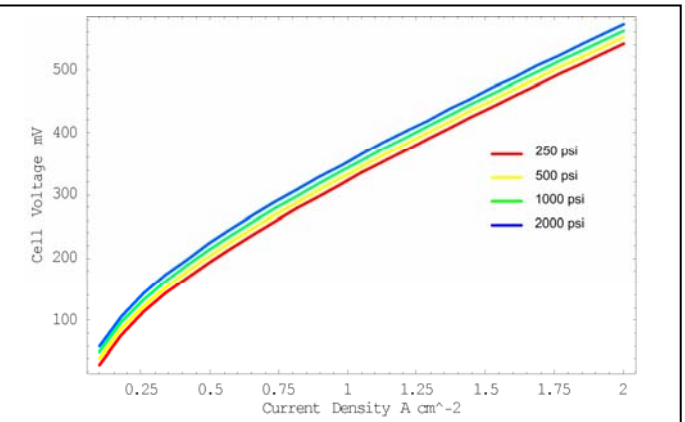

Figure 38: Cell voltage of PEM cell compressor at various product pressures.

***Comparison of Electrochemical and Mechanical Compression***

The calculation of the work required to

compress the hydrogen to the high storage pressure is complicated because of factors such as hydrogen does not behave as an ideal gas at high pressures and the compression process is done in stages with cooling between these stages. Many investigators consider compression of hydrogen as an isentropic process to simplify the calculations. They assume during compression there is no heat exchange between compressor and environment and the process is reversible. Since adiabatic hydrogen compression is not reversible process, isentropic compressor efficiency can be accounted for deviation from ideal behavior using an efficiency factor, approximately 75% -80% [xix]. Finally, the actual energy required by compressor (ie. electrical consumption) is calculated considering the mechanical efficiency of the compressor to be 90% [xix]. Figure 39 shows that mechanical compression requires more energy to compress the hydrogen gas at lower pressure ranges than at elevated pressure ranges. Mechanical compression is efficient for compressing gases from 2000 psi to 10000 psi, but not from atmospheric pressure to 2000 psi. This presents an opportunity for electrochemical compression.

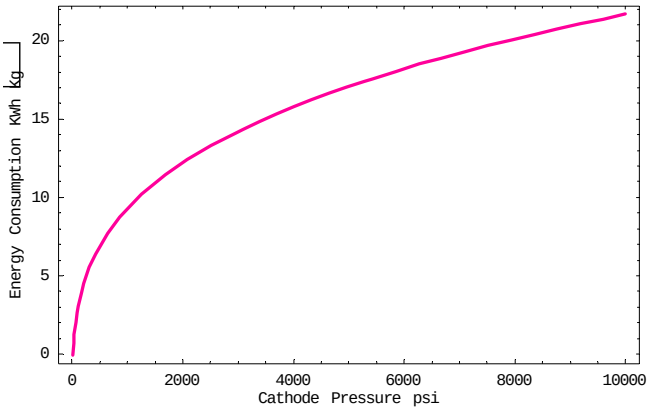

Figure 39: Energy consumption for mechanical compressor.

The work required for compression process was calculated at different current densities by multiplying the total cell voltage by current density and total active area. The calculations were done for a current density of 0.7 A/cm$^2$ and active area of 30 cm$^2$. The anode pressure is assumed to be constant at 14.7 psi. The calculations were done for an inlet hydrogen flow rate of 4 kg/h. To account for real time losses the efficiency of PEM cell compressor is assumed to be 70%. Calculated energy consumption for both mechanical and electrochemical compression for a product pressure range up to 2000 psi is shown in figure 40. The energy consumption for electrochemical compression is lower than for mechanical compression for most of the pressure range. Therefore, the efficient electrochemical compressor can serve as an intermediate step between electrolyzer and mechanical compressor to increase the whole system efficiency. Electrochemical compression can also reduce the number of compression and cooling stages resulting in more efficient compression process.

To compress the hydrogen from atmospheric pressure to 10000 psi using mechanical compression alone theoretically requires 22 KWh/Kg of $H_2$ as shown in figure 39. Calculations showed that electrochemical compression requires 7.5 KWh/Kg of $H_2$ energy to compress hydrogen from atmospheric pressure to 2000 psi. If electrochemical compression is used as an

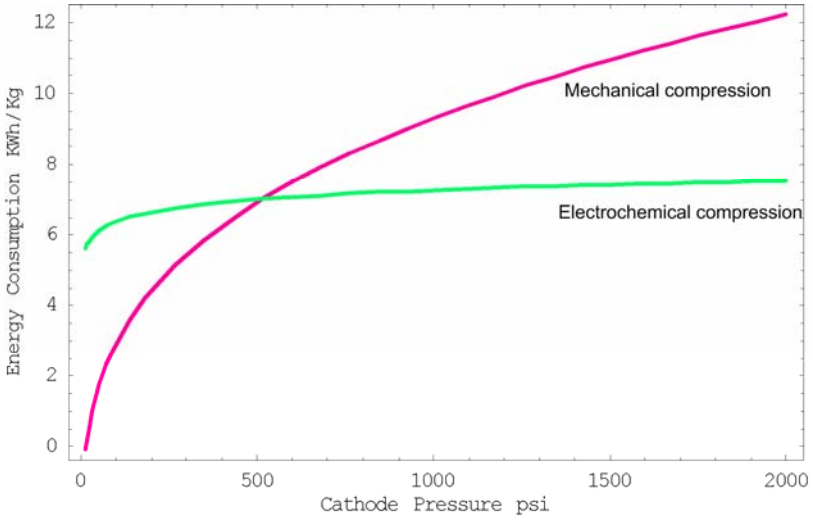

Figure 40: Comparison of energy consumption by mechanical and electrochemical compressor.

intermediate step between electrolyzer and mechanical compression to compress hydrogen upto 2000 psi and then mechanical compression from 2000 psi to 10000 psi, the energy saving is estimated as 5 KWh/Kg (~25%) according to theoretical calculations. The energy required for cooling stages during mechanical compression have not been considered for these calculations, and therefore, the energy savings from electrochemical compression are expected to be significantly higher.

***Future Electrochemical Compression Studies***

An experimental setup for electrochemical compression of hydrogen from PEM electrolyzer system planned for installation is shown in figure 41. The membrane of the electrochemical cell must be well hydrated to maintain the ionic conductivity; hence the hydrogen must be humidified before feeding to the anode. This can be achieved by using the product hydrogen gas from the PEM electrolyzer system, conditioned to compress electrochemically. The product hydrogen from PEM electrolyzer can be assumed to be 100% saturated. It is conditioned using a thermoelectric cooling system to the required humidity level to electrochemically compress using a PEM cell assembly [xx].

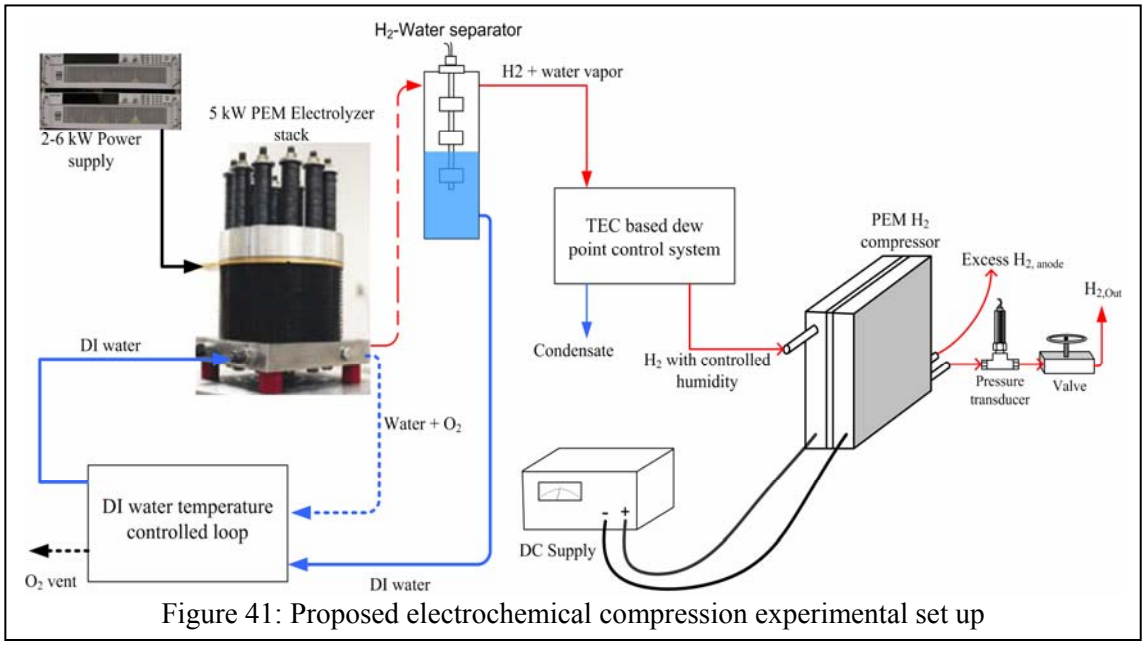

Figure 41: Proposed electrochemical compression experimental set up

3. *Continuation of the relationship between UND, NREL, EERC, and the North Dakota State Energy Office working towards wind to electrolyzer power and control design strategies.*

As a part of the project kick off activities, five members of the UND team, the two faculty and three Ph.D. students, visited NREL's NWTC to discuss and coordinate project goals. Meetings were held with leaders from both the wind and hydrogen groups and the associatd experimental facilities were visited. The result of the visit was a refinement of UND's project goals to align them more closely with those of DOE.

A project review meetings were held with the ND State Energy Office. The State Energy Office is interested in the results of the project and the potential development of new wind technologies for application in our state. Team members met on a periodic basis with the research managers of EERC's wind and hydrogen programs.

A doctoral candidate worked at the NREL site in May 2003 through January 2004, May 2004 through September 2004, and May 2005 through July 2005. During this time results of the testing were analyzed and the design and fabrication of the power electronics completed. Analyzing the data from the electrolyzer characterization allowed the joint NREL/UND team to best design and optimize the power electronics to directly interface a wind turbine directly to the PEM stack and/or the AC grid. This graduate now works for NREL.

4. *Collaborative relationships with industrial, academic, and public leaders in electrolysis, wind, hydrogen, and fuel cell systems.*

Members of the UND team visited Proton Energy Systems in December 2004 and initiated team-building relationships with this manufacturer. Several joint proposals have been written. NREL researchers are invited to attend during this same period to allow the multiple stakeholders objectives to be addressed.

The PI for the project provided project briefings to Basin Electric Power Cooperative of North Dakota. Basin Electric operates two wind turbines near Minot, North Dakota and has initiated a project with DOE to install a large electrolysis unit and hydrogen fueling station at the Minot site. Of primary interest was the use of one of the team's PhD candidates to help model dynamic scheduling of the wind turbine to optimize its power output.

Dr. Mann is currently a member of the DOE Water Electrolysis Working Group.

5. *Students trained to meet current and future energy-related needs in a fast growing and vital energy segment.*

Funding from this program has provided support for five doctoral students, four undergraduate students, and one post doctoral fellow. In addition, the project has raised awareness of renewable energy within the school. This has resulted in increased interest and enrollment in renewable/sustainable energy courses being taught by the Electrical and Chemical Engineering Departments.

6. *Fundamental small-scale educational/research facility available for undergraduate and graduate students. This enhanced infrastructure along with the partnerships formed will enhance the capability of UND to conduct nationally competitive energy-related research and education.*

Two major new test facilities were built at UND as a result of this grant. These facilities have been and will continue to advance both the teaching and research mission at UND.

**UND's Renewable hydrogen production System**

The renewable hydrogen production test facility at UND consists of a 6 kW PEM electrolyzer system and two 1.2 kW PEM fuel cells. The electrolysis system (fig 42) is designed to allow the precise control over operating temperature, hydrogen system pressure, water resistivity, water flow, stack current and safety. Along with the temperature, pressure and current-voltage sensors, the main components of the system are a 6 kW PEM electrolyzer stack, hydrogen-water phase separator, two 6 kW Xantrex DC power

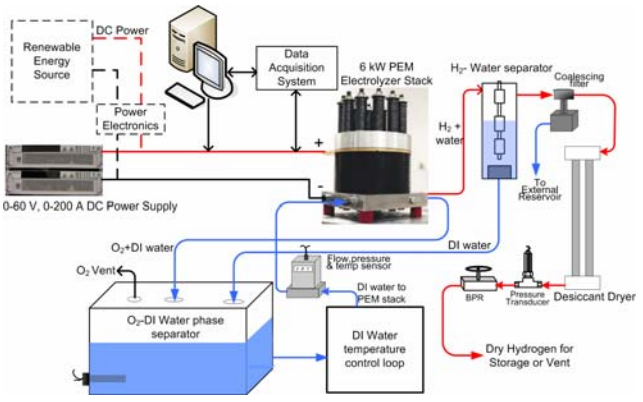


Figure 42. UND hydrogen test facility

supplies which are capable to deliver up to 200 A to the electrolyzer, a temperature controlled water loop, a two-tube desiccant drying system and a back pressure regulator to control the operating pressure. Water quality is maintained above the defined 1MΩ-cm using mixed bed resins and carbon filters. A temperature control unit (chiller) controls the inlet DI water temperature thereby providing control of the operating temperature of electrolyzer. This system is designed to allow higher temperature testing by maintaining DI water temperature with the chiller and a heater provided in oxygen-water phase separator.

**Electrochemical Impedance Spectroscopy**

EIS is a popular analytical tool whose results can be correlated with complex variables such as mass transport, charge transport, rates of chemical reactions, corrosion, dielectric properties, and effect of composition on the conductance. Very little work has been performed using EIS to analyze PEM electrolysis stacks because power supplies of required rating lack the wide frequency bandwidth required to conduct full range EIS studies. The primary limitation is a power system able to generate the high level of DC required to run the electrolysis stack at full load (140 A at 50 Volts) while applying the test signal (10 A at 0.01 to 20 kHz) required to perform the EIS analysis. Existing systems are typically restricted to either low current applications at the required frequency, or low frequency at the required current.

EIS studies of PEM cell stacks require a frequency response analyzer (FRA) supplying modulating signal to a DC power supply. The DC power supplies a base current and small AC perturbations are imposed on the PEM cell stack. The resulting voltage is measured and analyzed using FRA for different frequencies. Figure 43 shows the basic EIS experimental set up. A prototype of this system has been tested for a base DC up to 1A with AC signals up to 0.02 A and 300-4000Hz superimposed on the DC. The system generated output with no visual distortions over this frequency range. Our group plans to scale this system using their existing 200 A DC power supply and the Solartron frequency response analyzer.

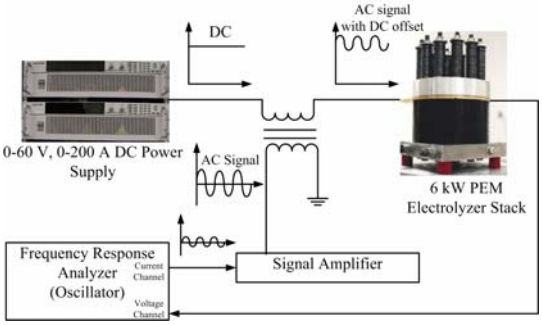

Figure 43. Prototyped EIS experimental schematic to be scaled up for proposed work.

7. *Project results disseminated through annual reports, peer-reviewed journals, conference presentations, undergraduate capstone design and/or term project reports, master's theses, and one or more dissertations detailing progress, barriers, lessons learned, and a path forward.*

The following papers, reports, and presentations have been given to disseminate the results of this work.

- Pacheco, E.H.; Biaku, C.; *Peters*, A.; Salehfar, H.; Mann, M.D.; "An Advanced PEM Fuel Cell Performance Prediction Model", *Journal of Power Sources*, **2005**, (in review).
- Harrison, K., Pacheco, E.H., Mann, M.D., and Salehfar, H.; "Semi-Empirical Model for Determining PEM Electrolyzer Stack Characteristics", *Journal of Fuel Cell Science and Technology*, **2005**, (in press).
- Harrison, K.; Mann, M.D.; *Salehfar*, H.; "Addressing System Integration Issues Required for the Development of a Distributed Hydrogen Energy System", *Abstract and presentation at* AWEA Conference, Pittsburgh, PA, June 4-7, 2005.
- Biaku, C.; Pacheco, E.H.; Peters, A.; Harrison, K.; Mann, M.D.; Salehfar, H.; "Modeling of a PEM Fuel Cell Performance", *Poster presented at* Living the Life of the Mind – Fourth Annual Scholarly Activities Forum, Grand Forks, ND, March 22-24, 2005.

- Mann, M.D.; Salehfar, H.; Harrison, K.; Biaku, C.; Peters, A.; Nilesh, D.; "Addressing System Integration Issues Required for the Development of a Distributed Hydrogen Energy System", *Abstract at the 2005 DOE EPSCoR Conference*, Morgantown, WV, June 12-14, 2005.
- Harrison, K.W.; Kroposki, B.; Pinl, C.; "Electrolyzer Characterization Report: Proton Energy Systems HOGEN 40RE"; October, 2005, NREL publication.
- Harrison KW, Hernandez-Pacheco E, Mann M, Salehfar H, Semiempirical model for determining PEM electrolyzer stack, *J.of Fuel Cell Science and Technology*, Vol. 3, May 2006, pp. 220-233.
- Biaku, C.Y.; Dale, N.V.; Mann, M.D.; Peters, A.J; Salehfar, H.; Han, T.; "A Semi-Emperical Study of the Temperature Dependence of the Anode Charge Transfer Coefficient of a 6-kW PEM Electrolyzer" *Int. Journal of Hydrogen Energy,* 2007, in review.
- Pacheco, E.H., Mann, M.D.; "Rational Approximations" *Journal of Power Sources* 2004 128 (1): 34-44
- Harrison, K.W.; Peters, A.J.; Biaku, C.Y.; Dale, N.; Mann, M.D., Salehfar, H.; "Hydrogen Dew Point Control Utilizing Thermoelectric Devices", International Journal of Hydrogen, (in review)
- Peters, R.R.; Muthumumi, D.; Bartel, T.; Salehfar, H.; Mann, M.D.; "Static VAR Compensation of a Fixed-Speed Stall Control Wind Turbine at Start-UP, IEEE Transactions (In review)
- Peters, R.R., Stevens, B.; Mann, M.D.; Salehfar, H.; "Dynamic Scheduling of Wind Energy for Hydrogen Production by Electrolysis", Published in Proceedings of 37th North American Sympoisium, October 23-25, 2005, Ames, IA.
- Peters, R.R.; Muthumuni, D.; Bartel, T.; Salehfar, H.; Mann, M.; "Dynamic Model Development of a Fixed Stall control Wind Turbine as Start-Up", Published in Proceedings of 2006 Power Engineering Society General Meeting, June 18-22, 2006, Montreal, Canada.
- Mann, M.D.; "Addressing System Integration Issues Required For The Development Of Distributed Wind-Hydrogen Energy Systems -1" U.S. Department of Energy (Grant No. DE-FG02-04ER46115), Department of Chemical Engineering, December 2005.
- Kroposki, J.; Levene, J.; Harrison, K.; Sen, P.K.; Novachek, F.; "Electrolysis: Information and Opportunities for Electric Power Utilities", NREL/TP-581-40605, September 2006.
- "Development of Distributed Wind-Hydrogen Energy System using PEM Electrolysis Stack"- Scholarly Forum, Grand Forks, ND, March 2006.
- " Modeling of a PEM Electrolyzer Performance"- Scholarly Forum, Grand Forks, ND, March 2006.
- " Addressing System Integration Issues Required For The Development of a Distributed Wind-Hydrogen Energy System" – AWEA WINDPOWER Conference May,2006
- "PEM Electrolysis System Design For Renewable Hydrogen Production"- Scholarly Forum Feb, 2007
- "Electrochemical hydrogen compression using PEM cell"- Scholarly Forum Feb, 2007
- "A Semi-Empirical Study of the Temperature Dependence of the Anode Charge Transfer Coefficient of a 6 kW PEM Electrolyzer" - Scholarly Forum Feb, 2007
- PEM Electrolysis Hydrogen Production System Design For Improved Testing And Optimization- NHA Annual Hydrogen Conference, San Antonio, March 2007 (Poster also)
- Electrochemical Compression Of Product Hydrogen From PEM Electrolyzer Stack- NHA Annual Hydrogen Conference, San Antonio, March 2007 (Poster also)
- Analysis of Impedance Data of a Partially Loaded 1.2 kW PEM Fuel Cell Stack- NHA Annual Hydrogen Conference, San Antonio, March 2007
- Electrochemical compression of hydrogen from renewable wind-PEM electrolysis generation systems- AWEA WINDPOWER Conference, Los Angeles, June 2007 (Poster also).
- A Study of Low Pressure Fuzzy Logic Wind Hydrogen System for Off-Grid Applications- AWEA WINDPOWER Conference, Los Angeles, June 2007 (Poster also)
- "Optimizing Power Electronics Systems for Wind to Hydrogen Generation System," Andrew J. Peters – *UND Scholarly Forum 2006 presented during Chemical Engineering's Highlights*.

- "Power Electronics Development for Wind to Hydrogen Generation System," Andrew J. Peters – *UND Graduate Seminar*, March 31, 2006.
- "Addressing System Integration Issues Required for the Development of a Distributed Wind-Hydrogen Energy System," Andrew J. Peters, Kevin W. Harrison, Nilesh V. Dale, Christian Y. Biaku, Dr. Michael D. Mann, and Dr. Hossein Salehfar – *AWEA WindPower 2006*
- "Hybrid Power System Model Development and Integration for Renewable Hydrogen Generation," Andrew J. Peters, Christian Y. Biaku, Nilesh V. Dale, Dr. Hossein Salehfar, Dr. Michael Mann, Tae-Hee Han. *UND Scholarly Forum 2007*.
- "Power Electronics for Interfacing of Wind Turbine and Electrolyzer for Hydrogen Generation," Andrew J. Peters, Christian Y. Biaku, Nilesh V. Dale, Dr. Hossein Salehfar, and Dr. Michael D. Mann – *AWEA WindPower 2007 (to be completed)*
- "Power Electronics for Interfacing of Wind Turbine and Electrolyzer for Hydrogen Generation," Andrew J. Peters, Christian Y. Biaku, Nilesh V. Dale, Dr. Hossein Salehfar, and Dr. Michael D. Mann – *AWEA WindPower 2007*
- "Hybrid Renewable Power System Development for Hydrogen Generation in RPM-Sim," – *in preparation*

**SIGNIFICANT FINDINGS / EVENTS / ACCOMPLISHMENTS**

Significant findings, events, and accomplishments are presented in bulleted for here. Specific details were presented in the "Progress Against Schedule / Milestones" section.

Developed fuel cell model for incorporation into NREL's RPMSim
- Open circuit voltage and terminal voltage from the geometry, operating conditions, load characteristics and the materials properties of the fuel cell
- Transient voltage response to changing loads
- Fault behavior (short circuit characteristics)
- Fuel cell stack parameters
- Thermal response / co-generation
- Water management
- Power output

Electrolyzer model completed
- Accurately predicts performance of Proton Energy's Hogen 40RE used at NREL
- Incorporates temperature, current, and voltage into model
- Predicts membrane specific constants from experimental data
- Modified for incorporation into RPMSim

Collaboration with NREL
- Doctoral student worked at NREL to install and test a 7kW proton exchange membrane electrolyzer at NREL's National Wind Technology Center
- UND's modeling coordinated with NREL to facilitate incorporation into RPMSim
- UND test facilities complement NREL's existing hydrogen test facility
- UND graduate of this program, Dr. Kevin Harrison currently employed in NREL's wind/hydrogen group

Research/education capabilities upgraded to support development of power electronics and control
- Fuel cell test facility configured around a 1.2 kW Ballard fuel cell
- Integrated electrolysis facility to gather fundamental information for the integration of the electrolyzer with the wind generator
- Eletrochemical Impedance Spectroscopy system will be used to develop equivalent circuit models

System development to improve electrolyzer performance and cost
- Novel method of drying hydrogen

- Power control system with lower energy losses
- Electrochemical compression being investigated

**STUDENTS SUPPORTED BY DOE**

This program has supported the following during this program:

- Five Ph.D. students
- Two undergraduate students
- One post doctoral fellow

**REFERENCES**


i M. Oszcipok, D.Reimann, U. Kronenwett, M. Kreideweis, M.Zedda, J.of Power Sources 145(2005) 407-415.

ii J. Amphlett, B. Peppley, E. Halliop, A. Sadiq, J.of Power Sources 96(2001) 204-213.

iii S Cleghorn, D. Mayfield, D.Moore, J.Moore, G. Rusch, T.Sherman, J.of Power sources 158 (2006) 446-454.

iv H. Song, D. Shin, Int. J. of Hydrogen Energy 26( 2001) 1259-1262.

v W. Zhu, R. Payne, B. Tararchuk, J. of Power Source 168 (2007) 211-217.

vi N. Wagner, E. Gulzow, J.of Power Sources 127(2004) 341-347.

vii X. Yuan, J.C. Sun, H. Wang, J. Zhang, J.of Power Sources 161 (2006) 929-937.

viii Princeton Applied Research, Basics of Electrochemical impedance spectroscopy, application note AC-1, 2005.

ix F. Jaouen, G. Lindbergh, G. Sundholm, J. Electrochem Soc. 149 (2002) A437-A447.

x J. Ihonen, F. Jaouen, G. Lindbergh, A. Lundblad,G. Sundholm, J. Electrochem Soc. 149 (2002) A448-A454

xi R. Makharia, M. Mathias, D. Baker, J. Electrochem Soc. 152 (2005) A970-

xii S.Roy, M. Orazem, B. Tribollet. J. Electrochem Soc. 154 ( 2007) B1378-B1388.

xiii M.L. Perry, J. Newman, E.J. Cairns, J. Electrochem. Soc. 145 (1998) 5–15.

xiv H.C. Young, G.S. Yong, C.C.Won, I.W. Seong, S.H. Hak, J. Power Sources 118 (2003) 334–341

xv T.J.P. Freire, E.R. Gonzalez, J. Electroanal. Chem. 503 (2001) 57–68

xvi V.A. Paganin, C.L.F. Oliveira, E.A. Ticianelli, T.E. Springer, E.R. Gonzalez, Electrochim. Acta 43 (1998) 3761–3766

xvii K.C. Neyerlin, Wenbin Gu,Jacob Jorne,H.A. Gasteiger: *Study of the exchange current density for the hydrogen oxidation and evolution reactions*, J. of Electrochemical Soc.2007 (154)

xviii K.W. Harrison, H. Pacheco, M.D. Mann, H Salehfar: *Semiempirical model for determining PEM electrolyzer stack*, J of Fuel Cell Science and Technology, 2006 (3)

xix E Tzimas, C Filiou, S.D Peteves : *Hydrogen Storage:State of the Art and Future Perspective*, European Commision, 2003

xx K. W. Harrison, A. J. Peters, C. Y. Biaku, N. V. Dale, M. D. Mann, H. Salehfar: *Hydrogen dew point control utilizing thermoelectric devices*, Int. J. of Hydrogen Energy, in review.

Ref from nilesh paper

xx M. Oszcipok, D.Reimann, U. Kronenwett, M. Kreideweis, M.Zedda, J.of Power Sources 145(2005) 407-415.

xx J. Amphlett, B. Peppley, E. Halliop, A. Sadiq, J.of Power Sources 96(2001) 204-213.

xx S Cleghorn, D. Mayfield, D.Moore, J.Moore, G. Rusch, T.Sherman, J.of Power sources 158 (2006) 446-454.
xx H. Song, D. Shin, Int. J. of Hydrogen Energy 26( 2001) 1259-1262.
xx W. Zhu, R. Payne, B. Tararchuk, J. of Power Source 168 (2007) 211-217.
xx N. Wagner, E. Gulzow, J.of Power Sources 127(2004) 341-347.
xx X. Yuan, J.C. Sun, H. Wang, J. Zhang, J.of Power Sources 161 (2006) 929-937.
xx Princeton Applied Research, Basics of Electrochemical impedance spectroscopy, application note AC-1, 2005.
xx F. Jaouen, G. Lindbergh, G. Sundholm, J. Electrochem Soc. 149 (2002) A437-A447.
xx J. Ihonen, F. Jaouen, G. Lindbergh, A. Lundblad,G. Sundholm, J. Electrochem Soc. 149 (2002) A448-A454
xx R. Makharia, M. Mathias, D. Baker, J. Electrochem Soc. 152 (2005) A970-
xx S.Roy, M. Orazem, B. Tribollet. J. Electrochem Soc. 154 ( 2007) B1378-B1388.
xx M.L. Perry, J. Newman, E.J. Cairns, J. Electrochem. Soc. 145 (1998) 5–15.
xx H.C. Young, G.S. Yong, C.C.Won, I.W. Seong, S.H. Hak, J. Power Sources 118 (2003) 334–341
xx T.J.P. Freire, E.R. Gonzalez, J. Electroanal. Chem. 503 (2001) 57–68
xx V.A. Paganin, C.L.F. Oliveira, E.A. Ticianelli, T.E. Springer, E.R. Gonzalez, Electrochim. Acta 43 (1998) 3761–3766